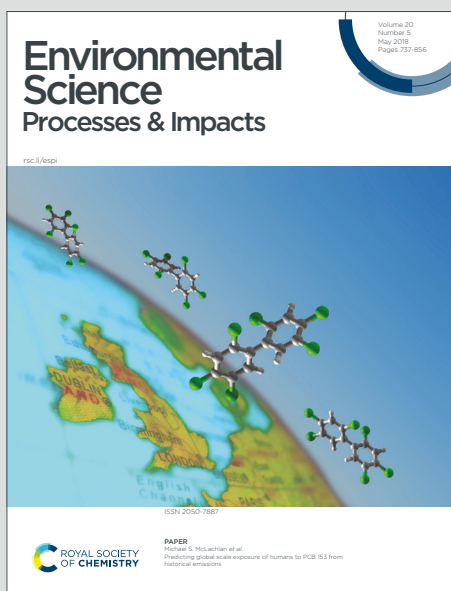


# Environmental Science Processes & Impacts

Accepted Manuscript

This article can be cited before page numbers have been issued, to do this please use: T. Matoušek, M. Prokopová, M. Pivokonsky and M. Filella, *Environ. Sci.: Processes Impacts*, 2026, DOI: 10.1039/D6EM00068A.



This is an Accepted Manuscript, which has been through the Royal Society of Chemistry peer review process and has been accepted for publication.

Accepted Manuscripts are published online shortly after acceptance, before technical editing, formatting and proof reading. Using this free service, authors can make their results available to the community, in citable form, before we publish the edited article. We will replace this Accepted Manuscript with the edited and formatted Advance Article as soon as it is available.

You can find more information about Accepted Manuscripts in the [Information for Authors](#).

Please note that technical editing may introduce minor changes to the text and/or graphics, which may alter content. The journal's standard [Terms & Conditions](#) and the [Ethical guidelines](#) still apply. In no event shall the Royal Society of Chemistry be held responsible for any errors or omissions in this Accepted Manuscript or any consequences arising from the use of any information it contains.

Environmental significance

Germanium has long been considered a geochemical twin of silicon and used to trace silicon-related processes such as rock weathering or ocean productivity. However, it has received little attention in freshwater biogeochemistry, partly due to analytical challenges. After developing and validating suitable methods, we studied germanium over a year in two contrasting reservoirs with different physical, chemical, and trophic conditions, including pollution legacies. Our results confirm that the presence of diatoms strongly influences inorganic germanium cycling. Methylated forms of germanium are also present, though at much lower concentrations, and their origin remains unknown. The ability to measure all these species now opens new questions about their environmental behaviour, especially as germanium gains attention as a technology-critical element.

1  
2  
3  
4  
5  
6  
7  
8  
9  
10  
11  
12  
13  
14  
15  
16  
17  
18  
19  
20  
21  
22  
23  
24  
25  
26  
27  
28  
29  
30  
31  
32  
33  
34  
35  
36  
37  
38  
39  
40  
41  
42  
43  
44  
45  
46  
47  
48  
49  
50  
51  
52  
53  
54  
55  
56  
57  
58  
59  
60

Open Access Article. Published on 26 March 2026. Downloaded on 4/16/2026 6:03:14 AM.  
This article is licensed under a Creative Commons Attribution 3.0 Unported Licence.



Environmental Science: Processes & Impacts Accepted Manuscript

1  
2  
3 Seasonal speciation of dissolved germanium in Bohemian reservoirs with  
4 contrasting chemistry and trophic status  
5  
6

7  
8 Tomáš Matoušek<sup>a</sup>, Michaela Prokopová<sup>b</sup>, Martin Pivokonský<sup>b</sup>, Montserrat Filella<sup>c,\*</sup>  
9  
10

11  
12  
13  
14  
15  
16  
17  
18  
19  
20  
21  
22  
23  
24  
25  
26  
27  
28  
29  
30  
31  
32  
33  
34  
35  
36  
37  
38  
39  
40  
41  
42  
43  
44  
45  
46  
47  
48  
49  
50  
51  
52  
53  
54  
55  
56  
57  
58  
59  
60

<sup>a</sup>Institute of Analytical Chemistry of the Czech Academy of Sciences, Veveří 97, 602 00 Brno,  
Czech Republic

e-mail: matousek@iach.cz ORCID number: 0000-0002-7603-1773

<sup>b</sup>Institute of Hydrology of the Czech Academy of Sciences, Pod Pat'ankou 30/5 160 00 Prague 6,  
Czech Republic

e-mail: prokopova@ih.cas.cz ORCID number: 0000-0002-1731-3551

e-mail: pivo@ih.cas.cz ORCID number: 0000-0003-2067-2632

<sup>c</sup>Department F.-A. Forel for environmental and aquatic sciences, University of Geneva,  
Boulevard Carl-Vogt 66, CH-1205 Geneva, Switzerland

e-mail: montserrat.filella@unige.ch ORCID number: 0000-0002-5943-1273

## Abstract

Although germanium is increasingly important for modern technologies, its occurrence and biogeochemical behaviour in natural waters remain insufficiently characterized, particularly in freshwater environments; here we investigate its speciation and seasonal dynamics in two contrasting drinking water reservoirs. The speciation of dissolved germanium, including inorganic, methyl-, and dimethyl-germanium, was monitored monthly over the course of a year in two drinking water reservoirs. The sampling covered both the productive and winter periods. The study sites were Vrchlice, a eutrophic reservoir in Central Bohemia that becomes anoxic in summer, and Souš, an oligotrophic reservoir in the mountainous region of North Bohemia, which was historically affected by acid rain. Speciation was measured using hydride generation–cryotrapping–inductively coupled plasma–mass spectrometry (HG-CT-ICP-MS/MS). The two reservoirs showed markedly different concentrations of inorganic Ge (iGe). In winter, before snowmelt, iGe concentrations were  $3.1 (\pm 0.1) \text{ ng L}^{-1}$  in Vrchlice and  $21.3 (\pm 0.3) \text{ ng L}^{-1}$  in Souš. Throughout the year, in Vrchlice iGe developed nutrient-type vertical profiles resembling those of silicon, consistent with the presence of diatoms. In contrast, no such pattern was observed in Souš, where diatoms were absent. Both reservoirs showed evidence of Ge fluxes from sediments during summer. Methylated Ge species exhibited conservative behaviour. In Vrchlice, average concentrations were  $0.34 \text{ ng L}^{-1} (\pm 0.04)$  for methylgermanium and  $0.09 \text{ ng L}^{-1} (\pm 0.02)$  for dimethylgermanium. In Souš, concentrations, were lower, with methylgermanium near the limit of quantification at  $\sim 0.07 \text{ ng L}^{-1}$ , and dimethylgermanium below detection limit. These findings are consistent with earlier observations from Lake Geneva. They confirm that freshwater systems lack an apparent *in situ* source of methylated Ge species, and that the inorganic form dominate, in contrast to marine environments.

## Keywords:

Vrchlice; Souš; drinking water reservoirs; methylgermanium; dimethylgermanium; freshwaters

## Introduction

Germanium (Ge), a group 14 element in the Periodic Table, is gaining economic importance due to its critical role in advanced technologies.<sup>1,2</sup> Its main global applications include electronics, solar technologies, fiber-optic systems, infrared optics, and polymerization catalysts.<sup>3</sup> Despite its growing technological relevance and its release into the environment through processes such as coal combustion, the environmental behaviour of germanium remains poorly understood, limiting our ability to assess its fate in natural systems. A recent comprehensive review of germanium's presence in environmental compartments<sup>4</sup> highlights significant gaps in our understanding, particularly outside of riverine and marine systems.

In rivers, research has focused on germanium's substitution for silicon in silicate minerals, offering insights into silicate weathering. In oceans, its chemical similarity to silicon has made it a valuable proxy in studying the silicon cycle, which plays a key role in both ocean ecology and the global carbon cycle. Dissolved inorganic germanium (iGe) concentrations in seawater closely correlate with dissolved silica, reflecting uptake by diatoms and other biosilicifiers. In addition to iGe, germanium also occurs in methylated forms, which exhibit markedly different behaviour. While iGe shows a nutrient-like distribution, monomethyl (MGe) and dimethyl germanium (DMGe) are largely inert both biologically and chemically, and typically display vertical profiles. These methylated species are more abundant than iGe in seawater, yet their sources remain uncertain. Proposed origins include microbial activity in sediments<sup>5</sup>, hydrothermal vents, and riverine inputs.<sup>6,7</sup>

In contrast to marine systems, germanium behaviour in lakes is much less studied, particularly with respect to its methylated forms. This knowledge gap likely arises from analytical challenges, as concentrations frequently approach or fall below detection limits. Nevertheless, studying germanium dynamics in lakes could provide valuable insights into silicate weathering, ecosystem productivity, and the role of microbial or sedimentary processes in its cycling. To help fill this gap, and building on our previous study in Lake Geneva,<sup>8</sup> we investigated germanium speciation over a year in two Bohemian drinking water reservoirs with contrasting chemical and trophic conditions. Unlike Lake Geneva, the largest lake in Western Europe with a surface area of 580.1 km<sup>2</sup> and a volume of 89 km<sup>3</sup>, these two reservoirs are considerably smaller and differ markedly

1  
2  
3 from each other (Table 1). Vrchlice, located in Central Bohemia, is a eutrophic reservoir that  
4 becomes anoxic in summer. In contrast, Souš, situated in North Bohemia, is oligotrophic, and has  
5 been significantly impacted by acid rain (Figure 1).  
6  
7

8  
9 Following common practice in environmental sciences, concentrations are expressed in gram units  
10 except when calculating molar ratios.  
11

## 12 Systems studied

### 13 Vrchlice reservoir


14 The Vrchlice reservoir catchment, covering approximately 97 km<sup>2</sup>, is located in the Czech  
15 Republic (Figures 1 and SI1a). The highest point of the basin reaches 555 m AMSL, while the  
16 lowest point –the reservoir outlet is at 308 m AMSL. Built in 1970 to supply drinking water to the  
17 nearby town of Kutná Hora, it holds 7.9 million m<sup>3</sup> of water and serves more than 50,000  
18 inhabitants in the surrounding area.<sup>9</sup> The area is characterized as moderately warm and moderately  
19 humid, with an average annual temperature of 9 °C, and annual precipitation of 550-600 mm  
20 (<https://www.chmi.cz/namerena-data/historicka-data/mapy-srazkovych-uhru>). More than half of  
21 the catchment area is covered by arable land, with wheat, rapeseed, maize, and barley as the main  
22 crops. In recent years, increased sedimentation has been observed in the reservoir, a process that  
23 has been the focus of several studies.<sup>10,11</sup>  
24  
25  
26  
27  
28  
29  
30  
31  
32  
33  
34  
35  
36  
37  
38  
39  
40  
41  
42  
43  
44  
45  
46  
47  
48  
49  
50

51 The bedrock of the Vrchlice reservoir and its catchment consists primarily of Variscan-age  
52 gneisses, micaschists, and migmatites, with local occurrences of Upper Cretaceous sandstones.  
53 The reservoir is located near the southern section of the Kutná Hora polymetallic ore district, which  
54 exhibits anomalous Ag-Sb mineralization along its southern margin, including minor occurrences  
55 of arsenic and germanium.<sup>12</sup> However, this mineralization is located approximately 2 km  
56 downstream to the west of the reservoir and does not influence the chemical composition of its  
57 waters.  
58  
59  
60

### 61 Souš reservoir

62 The Souš Reservoir is located on the Černá Desná River in the highest part of the Jizerské  
63 Mountains, Czech Republic (Figures 1 and SI1b). The river originates north of the reservoir at an  
64  
65  
66

Open Access Article. Published on 26 March 2016. Downloaded on 16/12/2016 16:05:11. This article is licensed under a Creative Commons Attribution 3.0 Unported Licence.




altitude of approximately 880 m AMSL, in a valley between the Jizera (1122 m AMSL) and Černý vrch (1,025 m AMSL) hills. The average annual temperature in Souš is 5.6 °C, and between May 2023 and April 2024 a total of 1575 mm of precipitation was recorded.<sup>13,14</sup> The reservoir serves primarily for drinking water supply and flood mitigation in downstream areas. Its construction, along with other dams in the Kamenice River basin, was prompted by repeated floods in the early 20th century (1888, 1897, 1907), which seriously affected the developing glass industry. The Souš dam was built between 1911 and 1915, together with the Bílá Desná dam in a neighbouring valley. Following the catastrophic breach of the Bílá Desná dam in 1916, the Souš dam was re-evaluated for safety and reconstructed between 1924 and 1927. Until the 1960s, the reservoir was used for recreational purposes. However, growing demand for drinking water in the Jablonec, Tanvald and Železný Brod regions led to a reconstruction between 1969 and 1974, converting the Souš reservoir into a dedicated water supply source. As a result, swimming and fishing were prohibited, and the surrounding area is now strictly protected.

To support the reservoir's hydrological balance, part of the flow from the neighbouring Bílé Desná basin can be diverted into the Souš reservoir. Water is channelled through a concrete pipe from the Bílá Desná River, then through a 1,145 m long gallery to an unnamed tributary feeding the reservoir. Two underdrains, located in a tunnel excavated into the left rocky slope, serve to drain the water from the reservoir.

The Jizerské Mountains, part of the so-called “Black Triangle”, were among the first and most heavily impacted areas globally by acid atmospheric deposition. Anthropogenic acidification, likely beginning as early as the mid-1940s, severely affected surface waters and watersheds on the upper plateau.<sup>15</sup> The granite bedrock and shallow podzolic soils in the region are particularly vulnerable to acidification. By the 1980s, nearly the entire Souš reservoir basin had been deforested, resulting in increased transport of organic matter and elevated aluminium concentrations. These conditions, especially during spring thaw, made it difficult to treat the cold, acidic water to meet drinking water standards. To improve water treatment, aerial liming of the reservoir was carried out each spring between 1996 and 2015.<sup>16</sup> Today, the watershed is once again fully forested.

1  
2  
3  
4  
5  
6  
7  
8  
9  
10  
11  
12  
13  
14  
15  
16  
17  
18  
19  
20  
21  
22  
23  
24  
25  
26  
27  
28  
29  
30  
31  
32  
33  
34  
35  
36  
37  
38  
39  
40  
41  
42  
43  
44  
45  
46  
47  
48  
49  
50  
51  
52  
53  
54  
55  
56  
57  
58  
59  
60

Open Access Article. Published on 26 March 2026. Downloaded on 16/2/2026 6:03:14 AM.  
This article is licensed under a Creative Commons Attribution 3.0 Unported Licence.



## Materials and methods

### Sampling

Monthly depth profile sampling was conducted at the deepest points of the reservoirs. In Vrchlice, this was at the dam, approximately in its centre (49.9270392N, 15.2270806E). In Souš, samples were collected from a boat on the north side of the intake tower (50.7911378N, 15.3183094E). The specific dates and times of sampling are provided in the Supporting Information Excel file.

In addition, samples were taken from the tributaries of the Vrchlice and Souš reservoirs at three points each (IV1–IV3) and (IS1–IS3) on 14 and 15 May 2024, respectively; see Figures SI1a and SI1b.

A complete overview of the sampling and preservation strategies used for all analyses is shown in Figure SI2. Physical parameters were measured *in situ* using a multimeter probe HI 98494 (Hanna Instruments; Czechia) for pH (accuracy  $\pm 0.02$  pH), ORP ( $\pm 1.0$  mV), conductivity ( $\pm 1 \mu\text{S cm}^{-1}$ ), dissolved oxygen ( $\pm 0.1\%$ ), and temperature ( $\pm 0.15$  °C). Water samples were collected using a Ruttner water sampler (2theta; Czechia). Aliquots for laboratory analysis of hydrochemical parameters were collected in 1 L polyethylene bottles pre-cleaned with acid and analysed the same day. For trace element analysis by ICP-OES (Agilent 5110 Series, Agilent Technologies, USA) and for Ge, As and Sb speciation analysis, sample aliquots were filtered *in situ* using  $0.45 \mu\text{m}$  syringe filters (Macherey-Nagel regenerated cellulose, CHROMAFIL Xtra RC-45/25), previously validated for fast filtration and non-detectable blanks. Filtrates were collected in polypropylene centrifuge vials (Roth) and preserved by adding  $150 \mu\text{L}$  of  $0.2 \text{ M Na}_2\text{EDTA}$  (Sigma) per  $15 \text{ mL}$  of sample. Two additional aliquots were preserved by adding  $100 \mu\text{L}$  of concentrated  $\text{HNO}_3$  per  $15 \text{ mL}$  of sample.<sup>17</sup> For ICP-OES analysis, samples were diluted 1:1 by 1%  $\text{HNO}_3$ . Note that silicon was measured by ICP-OES and is not colorimetric “soluble silica”. All preserved samples were stored at  $4^\circ\text{C}$  in the dark.

### Ancillary data

Supplementary monthly data, including temperature, pH, conductivity, concentration of oxygen, nutrients, natural organic matter, and various chemical elements, for both reservoirs are provided

1  
2  
3  
4  
5  
6  
7  
8  
9  
10  
11  
12  
13  
14  
15  
16  
17  
18  
19  
20  
21  
22  
23  
24  
25  
26  
27  
28  
29  
30  
31  
32  
33  
34  
35  
36  
37  
38  
39  
40  
41  
42  
43  
44  
45  
46  
47  
48  
49  
50  
51  
52  
53  
54  
55  
56  
57  
58  
59  
60

in the Supplementary Excel file. The file also includes information on the corresponding experimental methods.

Additional environmental data were provided by the reservoir manager Povodí Labe, state enterprise (PLA). These include bathymetry, water levels and renewal, temperature, dissolved oxygen, and chlorophyll *a* (Chl *a*) profiles for 2022–2024, as well as integrated phytoplankton data based on species counts and biomass. Profiles of temperature, dissolved oxygen, and Chl *a* were recorded at ten sampling points in Vrchlice (yellow points in Figure SI1a) and three in Souš (yellow points in Figure SI1b). Graphical representations of these profiles, with sampling dates, are shown in Figures SI3. Integrated phytoplankton data correspond to profile 10 in Vrchlice and profile 3 in Souš, with sampling dates indicated in the corresponding figure.

### Germanium analysis

Samples were analysed for Ge species using a multi-elemental method that also enables the measurement of As and Sb species. The method is based on hydride generation (HG), followed by cryotrapping (CT) capture in a U-tube under liquid nitrogen, and detection by inductively coupled plasma tandem mass spectrometry (ICP-MS/MS). A detailed description, validation and discussion of the analytical aspects can be found in Matoušek et al. (2026).<sup>17</sup> All experimental parameters and ICP-MS/MS settings used in this study were identical to those reported there. For each series, limits of detection (LOD) values were calculated based on the actual blank variability. The LOD ranges were as follows: 0.04–0.2 ng L<sup>-1</sup> for iGe, 0.01–0.1 ng L<sup>-1</sup> for MGe, and 0.01–0.09 ng L<sup>-1</sup> for DMGe. Method blank concentrations ranged from 0.3–0.5, 0.04–0.14, and 0.07–0.30 ng L<sup>-1</sup> for iGe, MGe, and DMGe, respectively. The precision of the analysis ( $n = 8$ ) was 3% (at a concentration of 2.6 ng L<sup>-1</sup>) for iGe, 5% (0.3 ng L<sup>-1</sup>) for MGe and 5% (0.3 ng L<sup>-1</sup>) for DMGe.<sup>17</sup> Values below the limit of quantification (LOQ) were included in both calculations and graphs but are marked in red in the Supplementary Information Excel file. As a quality control measure, a certified river water sample (SLRS-6) from the National Research Council of Canada was included in each series of Ge speciation analyses. The mean concentration of iGe was  $6.8 \pm 0.3$  ng L<sup>-1</sup> (mean and standard deviation of 15 analyses across different days), which matches the value obtained in our previous study.<sup>8</sup> Methylated Ge species were below the LOD in SLRS-6.

Analyses were performed using two aliquots of EDTA-stabilised samples. Inorganic Ge was determined without pre-reduction within 1–4 days after sampling to avoid from the slow formation of the iGe–EDTA complex.<sup>17</sup> Methylated species (MGe and DMGe) were analysed in aliquots treated with L-cysteine, between 3–8 days after sampling (with two exceptions: 10 and 17 days in June and December 2023, respectively).

Some selected samples were reanalysed using a single-element method (hereinafter referred to as the ‘Ge-specific method’) with HG conditions specifically adjusted for the analysis of Ge speciation and with identical CT and ICP-MS/MS detection as described in detail in reference 18. The samples were measured in a single aliquot with the reaction modifier L-cysteine present in a cleaned-up buffer, rather than adding it to each sample. This reduces blank concentrations and variability, resulting in a better LODs: 0.04 ng L<sup>-1</sup> for iGe, 0.004 ng L<sup>-1</sup> for MGe and 0.016 ng L<sup>-1</sup> for DMGe.

## Results and discussion

The results are presented in two ways: depth profiles (Figures 2 and 3) and box-and-whisker plots (Figures SI4 and SI5). While box and whisker plots are not commonly used in this type of study, they provide a convenient visual tool for comparing monthly variations and assessing the conservativeness of each parameter (i.e. the degree to which data cluster in a given month). This visualization complements the depth profiles and was generated using the corresponding Excel function.

Due to seasonal changes in total water volume, stock calculations were performed for germanium, silicon and iron (Figures 4 and SI6). These calculations were based on lake bathymetry, dividing the water column into depth layers, each aligned with a discrete sampling interval containing a single measured concentration. Within each layer, the concentration was assumed to be uniform. The mass of each substance per layer was determined by multiplying the concentration by the layer’s volume, and the total stock was calculated by summing the masses across all layers.

All depth values in the profiles are referenced from the water surface (0 m), regardless of fluctuations of water level. As a result, in some sampling campaigns, bottom sampling points fell below the actual water column and disturbed the sediments in Vrchlice, causing sharp increases in

turbidity and other parameter values. These are noted in the Supporting Information Excel file highlighted in grey and have not been included in the figures.

### Setting the context: physical and chemical characteristics of the reservoirs' waters

In Vrchlice (Figure 2), stratification was already evident in the first sampling in May 2023, with a thermocline between 2.5 and 5 m. Surface temperatures rose through June and July, then declined, with a sharp drop between October and November. The reservoir was fully mixed only in December 2023 (4.7 °C throughout the water column) and February 2024 (3.6 °C), while stratification had begun to re-establish by March. No sampling was carried out in January 2024 due to ice cover, although the water column was known to be fully mixed at that time. In Souš, stratification was less pronounced (Figure 3). Temperature decreased gradually with depth, with no clear boundary between epilimnion and hypolimnion –likely due to the reservoir's shape and relatively shallow depth, which promote mixing. Sampling in Souš was not possible from December 2023 to April 2024 due to ice, snow, and safety constraints. The only confirmed instance of full mixing occurred in November 2023, with a uniform temperature of 7.0 °C throughout the column. Although the PLA monitoring data were not collected on the same days as ours, they provide valuable spatial context on the reservoir ensemble. In particular, temperature profiles from multiple locations during 2022, 2023 and 2024 support the representativeness of our depth profile measurements at site 10 in Vrchlice and site 3 in Souš.

Relatively constant water volumes are maintained in both Vrchlice and Souš. During periods of high inflow, such as snowmelt or heavy rainfall, much of the reservoir water is rapidly replaced. This rapid renewal can significantly affect the concentrations of chemical species and must be considered when interpreting their annual cycles. Figures 4a and 4b show the water levels on sampling dates and the 20-day water renewal for both reservoirs. A 100% renewal value indicates that the entire reservoir volume was replaced at least once in the previous 20 days. In both 2023 and 2024, near-complete water renewal occurred during the winter months and during isolated heavy rainfall events. The timing of these events varied: April–May in 2023, and September–October in 2024. By contrast, snowmelt occurs every winter, though with varying intensity. But, even snowfall patterns can differ greatly. For example, in Souš, where snow cover typically lasts from early November to late March, the 2023–2024 season saw a complete melt during a rainy

1  
2  
3 period in early February, with no significant snowfall accumulation for the remainder of the  
4 winter.<sup>14</sup>  
5

6  
7 Therefore, from a physical perspective, three distinct situations occur in both reservoirs, resulting  
8 in varying physical and chemical conditions that must be considered to understand the behaviour  
9 of germanium. From spring to autumn, thermal stratification develops –though it remains  
10 incomplete in Souš – and is accompanied by a significant decrease in water volume, likely due to  
11 drinking water extraction and the maintenance of ecological flow in the river. In December,  
12 complete mixing of the water occurs in Vrchlice, followed by an almost total renewal of the  
13 reservoir water during winter. In Souš, however, the mixing in November coincides with  
14 substantial water renewal, making it difficult to distinguish the effects of each process, unlike in  
15 Vrchlice, where the two can be separated more clearly  
16

17  
18 The two reservoirs show markedly different chemical characteristics. Conductivity, which broadly  
19 reflects inorganic ion content, highlights this contrast. In Souš (Figure SI5), conductivity remains  
20 low and stable around 25  $\mu\text{S cm}^{-1}$ , with a small drop in January. In Vrchlice (Figure SI4), values  
21 are much higher ( $\sim 390 \mu\text{S cm}^{-1}$ ), though a similar seasonal decrease is observed. The differences  
22 in conductivity reflect contrasting geology: Souš drains a granitic basin, producing very soft water,  
23 while Vrchlice drains a carbonate-rich catchment. Corresponding calcium concentrations support  
24 this: in Vrchlice averages 34  $\text{mg L}^{-1}$  (range: 29–42) while Souš has a mean of 1.5  $\text{mg L}^{-1}$  (range:  
25 1.1–1.9) (Figures SI4 and SI5).  
26

27  
28 pH values also differ between the reservoirs. In Vrchlice, pH reflects carbonate buffering, with  
29 vertical variations linked to photosynthesis in the epilimnion ( $\text{OH}^-$  production) and algal  
30 mineralisation in the hypolimnion ( $\text{H}^+$  production) (Figure SI4). In Souš, pH values are more acidic  
31 (5.6–7.0), consistent with its geology and acidification history (Figure SI5). In both systems,  
32 winter inflows correspond to noticeable pH decreases.  
33

34  
35 Natural organic matter (NOM) composition differs between the two reservoirs, as indicated by  
36 SUVA (specific UV absorbance) values. SUVA, which correlates with NOM aromaticity,<sup>19</sup>  
37 provides an estimate of the humic character of NOM. Higher values were observed in Souš  
38 (3.6  $\text{L mg}^{-1} \text{m}^{-1}$ ) than in Vrchlice (1.9  $\text{L mg}^{-1} \text{m}^{-1}$ ), see Supporting Information Excel file, likely  
39 reflecting the humic-rich catchment in Souš, which includes deciduous forests and swampy soils.  
40  
41  
42  
43  
44  
45  
46  
47  
48  
49  
50  
51  
52  
53  
54  
55  
56  
57  
58  
59  
60

1  
2  
3  
4  
5  
6  
7  
8  
9  
10  
11  
12  
13  
14  
15  
16  
17  
18  
19  
20  
21  
22  
23  
24  
25  
26  
27  
28  
29  
30  
31  
32  
33  
34  
35  
36  
37  
38  
39  
40  
41  
42  
43  
44  
45  
46  
47  
48  
49  
50  
51  
52  
53  
54  
55  
56  
57  
58  
59  
60

SUVA values increased in both reservoirs during snowmelt and heavy rainfall events, though the effect was less pronounced in Souš. Similar trends have been reported elsewhere.<sup>20</sup>

Oxygen profiles (Figures 2 and 3) illustrate clear differences in biological productivity. Vrchlice shows a pattern typical of productive systems, with the oxycline aligning with the thermocline. During winter mixing (December to February), the entire water column remained oxic, although full oxygen saturation was never reached. In the productive season, oxygen levels in the epilimnion became supersaturated, while anoxia developed in the hypolimnion by August–September 2023 below 7.5 m. Anoxia extended deeper in October (below 10 m) and November (below 15 m). In contrast, the water column in Souš never became fully anoxic, consistent with its lower productivity. An overview of the oxygen concentration depth evolution in both lakes during the years 2022, 2023 and 2024 is shown in Figures SI3.

Phytoplankton biomass in Souš was low during the study period, ranging from 0.32 to 0.98 mg L<sup>-1</sup> (Supporting Information Excel file). Species composition (Figure 4a) showed a succession of taxa, with diatoms nearly absent: they represented only 2% of biomass in June 2024 (outside our sampling period) and 0.2% in June 2023. In Vrchlice, phytoplankton biomass was higher (0.80–2.7 mg L<sup>-1</sup>) (Supporting Information Excel file) and the composition was markedly different, with two pronounced diatom peaks in April: 63% of total biomass in 2023 and 66% in 2024 (Figure 4b). Historical data indicate that during Souš's acidification period, its phytoplankton community was dominated by Dinophyta (*Gymnodinium uberrimum*), with very low species richness,<sup>21</sup> similar to other strongly acidified lakes. According to Hořická et al.,<sup>15</sup> the first signs of biological recovery (e.g. return of *Daphnia longispina*) appeared in the early 1990s. Further development was influenced by liming (since 1996) and the reintroduction of salmonid fish (*Salvelinus fontinalis*) between 1991 and 1998. Species richness has since increased, but Souš remains a very low-productivity system. The lack of diatoms in Souš is intriguing since it cannot be explained by past acidity only, as diatom microfossils are well preserved in lake sediments and widely used to track acidification and recovery.<sup>22-24</sup> A plausible factor may be the elevated germanium concentrations. Germanium dioxide (GeO<sub>2</sub>) is a well-established diatom specific inhibitor, used in algal cultures to suppress diatom growth,<sup>25-27</sup> believed to disrupt silica frustule formation by competing with silicon for uptake via SIT transporters.<sup>28-29</sup> While concentrations in Souš are far lower than those used experimentally, persistent exposure may have chronically hindered diatom development.

Chlorophyll *a* concentrations are very different in both reservoirs (Figure SI3) and confirm the difference in productivity and phytoplankton observations. In Souš (2022–2024), values ranged from 0 to 19.7  $\mu\text{g L}^{-1}$  (median: 1.7  $\mu\text{g L}^{-1}$ ), with only three samples exceeding 15  $\mu\text{g L}^{-1}$ , indicating very low productivity. In contrast, Vrchlice recorded values from 0 to 101.7  $\mu\text{g L}^{-1}$  (median: 6.2  $\mu\text{g L}^{-1}$ ).

In Vrchlice, silicon concentrations, illustrated by both lake profiles (Figure 2) and box-and-whisker plots (Figure SI4), exhibited a pattern typical of a biologically scavenged element. During the productive season, silicon was taken up by siliceous algae, leading to depletion in the photic zone and accumulation in the hypolimnion. During the May–November period of 2023, the reservoir's water volume decreased by approximately 25% (Figure 4a), yet silicon stocks remained stable after an initial drop linked to the first diatom bloom (Figure SI4). This likely reflects either recycling of silicon within the water column or replenishment from Vrchlice inlet, effectively offsetting losses due to water abstraction. Following the extensive winter water renewal, silicon concentrations more than doubled, and the total stock tripled.

Iron in Vrchlice showed a different trend. From May to November, concentrations remained relatively stable, with some profile variation toward the end of the productive season, likely due to sediment fluxes (Figure SI4). However, between December and February, iron concentrations rose sharply, by a factor of 14. This spike may have resulted from soil runoff following heavy rainfall. Notably, when the Vrchlice inlet in Malešov was sampled, it contained 0.18  $\text{mg L}^{-1}$  of iron, substantially higher than the average concentration in the lake in December (0.016  $\text{mg L}^{-1}$ ).

In Souš, silicon displayed consistent vertical profiles throughout the year, showing no signs of biological uptake or internal lake sources. Such a pattern is consistent with the near absence of diatoms (Figure 3). Over the same May–November period, silicon concentrations rose steadily by about 20% (Figure SI5). Although the reservoir's water volume declined by around 25%, the total stock of silicon declined much less. These observations indicate a continuous input of silicon from the watershed. Supporting this, a concentration of 6.1  $\text{ng L}^{-1}$  was measured on the only occasion when an influent stream was sampled. In December, mixing combined with significant water renewal maintained similar silicon concentration, but with an increased total stock. Conversely,

1  
2  
3  
4  
5  
6  
7  
8  
9  
10  
11  
12  
13  
14  
15  
16  
17  
18  
19  
20  
21  
22  
23  
24  
25  
26  
27  
28  
29  
30  
31  
32  
33  
34  
35  
36  
37  
38  
39  
40  
41  
42  
43  
44  
45  
46  
47  
48  
49  
50  
51  
52  
53  
54  
55  
56  
57  
58  
59  
60

Open Access Article. Published on 26 March 2026. Downloaded on 4/16/2026 6:03:12 AM.  
This article is licensed under a Creative Commons Attribution 3.0 Unported Licence.



when large volumes of water were flushed from the reservoir, both silicon concentrations and total stock declined, pointing to an inflow of water with different chemical characteristics.

Iron in Souš followed a contrasting pattern. Throughout the May–November period, iron concentrations increased 3.2-fold (Figures 3 and SI5), and the shape of the vertical profiles suggested the gradual establishment of a sediment source in the hypolimnion. This developed under conditions of limited water mixing and oxygen depletion near the bottom. As a result, the iron stock increased approximately fourfold (Figure SI6), due to a combination of water loss and rising concentrations. In winter, after large volumes of water were flushed from the reservoir, both iron concentrations and stock dropped, by fourfold and fivefold, respectively.

### Inorganic germanium in the reservoir's waters

The concentrations of iGe differ markedly between the two reservoirs studied. Vrchlice displays concentrations typical of uncontaminated freshwater systems (Figures 2 and SI4), whereas values in Souš (Figures 3 and SI5) fall within ranges generally associated with geothermal environments or, in some cases, polluted systems.<sup>4</sup> Souš water has no geothermal origin, and there are no direct contamination sources such as mining or smelting activities. However, the reservoir was subjected for many years to severe acid rain pollution. Atmospheric deposition of coal fly ash, identified decades ago as a major anthropogenic source of Ge,<sup>30–35</sup> has since been confirmed by more recent studies.<sup>35</sup> Froelich et al.<sup>33</sup> estimated that more than two-thirds of riverine iGe originated from coal combustion. Although this figure may no longer reflect current global contributions, more recent studies suggest that coal remains an important Ge source in specific regions.<sup>36–37</sup> In the case of Souš, there is little doubt that past coal-related deposition has played a significant role as a germanium source.

Beyond differences in concentration, iGe also exhibits distinct behaviours in each reservoir. In Vrchlice, vertical profiles of iGe show patterns typical of a biologically active nutrient, closely mirroring those of silicon. This behaviour is similar to that observed in Lake Geneva<sup>8</sup> and in marine environments, where diatom uptake depletes both Si and Ge in surface waters, followed by their regeneration through dissolution or sediment diffusion at greater depths.<sup>4</sup> As previously noted, between May and November 2023, the water volume in Vrchlice decreased by approximately 25% (Figure 4a). Despite this reduction, the total iGe stock remained relatively stable, except for a

1  
2  
3 marked decline in June, which coincided with the diatom bloom. This suggests that, as with silicon,  
4 external or internal inputs of iGe compensated for losses due to outflow and biological uptake,  
5 resulting in a near steady-state condition. Interestingly, available data indicate that riverine iGe  
6 concentrations are similar to those within the reservoir, making inflow an unlikely explanation for  
7 reaching this balance in such a short period of time. Instead, sediment fluxes – evident in some  
8 vertical profiles– are a plausible source. Although disturbances during near-sediment sampling  
9 obscured natural gradients that could confirm *in situ* release and help estimate fluxes, the  
10 exceptionally high iGe concentrations recorded (often exceeding 25 ng L<sup>-1</sup>) strongly suggest that  
11 sediment interstitial waters serve as a significant iGe source to the water column. These disturbed  
12 samples also showed elevated silicon concentrations, though never more than twice the levels in  
13 the overlying water. Following the major water renewal event in winter, iGe concentrations  
14 remained constant –showing a behaviour notably different from that of silicon, and total iGe stock  
15 increased in proportion to the rise in water volume. Subsequently, iGe concentrations stabilized,  
16 and a new cycle began in spring, marked by another decline likely linked to biological uptake.  
17 Overall, iGe cycling in Vrchlice appears to be driven by a dynamic interplay of factors: diatom  
18 uptake during productive months, sedimentary release of iGe, minor riverine contributions, and  
19 seasonal hydrological changes.

20  
21  
22  
23  
24  
25  
26  
27  
28  
29  
30  
31  
32  
33  
34  
35  
36  
37  
38  
39  
40  
41  
42  
43  
44  
45  
46  
47  
48  
49  
50  
51  
52  
53  
54  
55  
56  
57  
58  
59  
60

In contrast to Vrchlice, Souš shows no signs of nutrient-like cycling. iGe concentrations increase progressively throughout the year, following a pattern similar to that of silicon, and without any evidence of biological uptake which is consistent with the absence of diatoms. Between August and October 2023, however, vertical profiles suggest an upward flux of germanium from sediments, a pattern not observed for silicon. This is likely driven by a concentration gradient between porewaters and the overlying hypolimnion under stable, unmixed conditions. Souš experienced a 25% decline in water volume between May and October 2023 (Figure 4b). If no significant inputs or losses of iGe had occurred, one would expect a similar 25% decrease in total stock. However, iGe stocks declined by only ~10%, while concentrations steadily rose (Figure 2). This indicates a net internal input of iGe, most plausibly from sediment release, since riverine iGe concentrations, when measured in May, were lower than those within the reservoir. From November 2023 to April 2024, a net loss of ~17 g of iGe was recorded. This likely reflects increased flushing due to rainfall or snowmelt, which overwhelmed internal inputs and transported iGe downstream. Under these conditions, iGe behaves more conservatively, governed by physical

hydrology and diffusion-driven sediment fluxes. Unlike Vrchlice, Souš lacks a strong diatom-driven biological pump. As a result, iGe is not regularly deposited into sediments through biological cycling. The sediment stocks that appear to release germanium at certain times of the year most likely reflect legacy accumulation, particularly from past periods of intense coal burning.

Similar enrichment patterns and vertical profiles of iron, observed from spring to autumn in Souš (Figures 3 and SI5) and, to a lesser extent, in Vrchlice (Figure SI4), raise the possibility of coupled Fe–iGe cycling. In Vrchlice, this may help explain the differing sediment release behaviour of germanium compared with silicon. One hypothesis is that iGe is sorbed onto iron oxyhydroxides and later released during reductive dissolution of iron under anoxic conditions in a process known in freshwater systems as the ‘iron wheel’.<sup>38</sup> While some studies support the sequestration of iGe in iron-rich phases during sediment diagenesis<sup>39–41</sup> and sorption onto iron hydroxides has been proposed as a control mechanism in rivers,<sup>34</sup> others report contradictory findings,<sup>42–43</sup> pointing instead to system-specific variability.

A principal component analysis (PCA) restricted to redox-sensitive variables (iGe, Fe, Mn, and dissolved oxygen) yields a dominant first component in Vrchlice (PC1  $\approx$  76% of the variance), with positive loadings for iGe, Fe, and Mn and a negative loading for O<sub>2</sub> (Figure SI7a). This reflects a clear redox gradient and corroborates the interpretation derived from the vertical profiles, namely that Ge is mobilised under reducing conditions together with Fe and Mn. In contrast, the same analysis applied to Souš shows a less coherent structure, indicating a more limited role of redox processes (Figure SI7b). PCA applied to variables such as iGe and Si does not provide additional insight, as it essentially reproduces the direct correlation already evident from the data and does not improve the mechanistic interpretation. For this reason, only the redox-focused PCA is retained as a complementary line of evidence.

### Ge/Si molar ratios

Ge/Si ratios have traditionally been used in two distinct geochemical contexts: marine productivity and continental weathering. In the oceans, the Ge/Si ratio is considered to be primarily controlled by the uptake of both elements by diatoms and other siliceous organisms. A value of  $\sim 0.7$   $\mu\text{mol mol}^{-1}$  is typically observed throughout the ocean water column, except in surface productive zones, where it becomes more variable, a variability often neglected in large-scale interpretations.<sup>43</sup> On

the other hand, in river systems, Ge/Si ratios are commonly interpreted in the context of chemical weathering. According to accepted models,<sup>45-46</sup> low-intensity weathering yields low dissolved Ge/Si values ( $\sim 0.35 \mu\text{mol mol}^{-1}$ ), as Ge remains largely retained in primary silicates. In contrast, high-intensity weathering, which leaches soils more completely, yields higher ratios (up to  $\sim 3.5 \mu\text{mol mol}^{-1}$ ) due to the congruent dissolution of secondary phases like clays.<sup>47-48</sup> In both marine and terrestrial contexts, the ratio is interpreted under the assumption that a single dominant process governs the Ge and Si cycles, either biological uptake or chemical weathering. However, this assumption breaks down in complex systems like freshwater reservoirs, where multiple processes act simultaneously.

In the Souš reservoir, where diatom activity is negligible, the Ge/Si ratio remains relatively stable around  $2 \mu\text{mol mol}^{-1}$  throughout much of the year (Figure SI5). At first sight, this could suggest an origin tied to rock and soil weathering, consistent with values expected from moderately leached catchments. However, the relatively high value is most probably due to the unusually high iGe concentrations linked to past accumulation during periods of intense atmospheric Ge deposition from coal combustion rather than to active soil processes. Moreover, during the summer months (July–September), when sediment-derived iGe fluxes increase (as shown in iGe concentration profiles), the Ge/Si ratio becomes more variable. This variability does not reflect a change in the weathering regime, but rather a fluctuation in iGe concentrations caused by internal reservoir processes such as release from the sediments, unrelated to contemporary weathering. In brief, in systems with significant non-weathering-related sources of iGe, such as sediment remobilization, the Ge/Si ratio can no longer be interpreted as a weathering proxy.

On the other hand, Vrchlice presents a different geochemical regime. Here, diatom uptake plays a significant role during productive months, resulting in low Ge/Si ratios ( $0.2\text{--}0.5 \mu\text{mol mol}^{-1}$ , Figure SI4). These values are in line with expectations for biological removal of Ge. However, in winter, large Si inflows not accompanied by corresponding Ge input sharply lower the Ge/Si ratio, again challenging a weathering-based interpretation when multiple processes are involved.

### **Methylated germanium in the reservoirs' waters**

The presence of methylated germanium species was confirmed in both Vrchlice and Souš reservoirs. In Vrchlice, MGe and DMGe exhibited conservative behaviour (Figures 5 and SI4),

with mean concentrations of  $0.34 \text{ ng L}^{-1}$  ( $\pm 0.04$ ) and  $0.09 \text{ ng L}^{-1}$  ( $\pm 0.02$ ), respectively. In contrast, in Souš, where the species also behaved conservatively, concentrations were lower: MGe was detected at approximately  $0.07 \text{ ng L}^{-1}$ , close to the quantification limit, while DMGe remained below detection. These values are substantially lower than those reported in oceanic waters but are consistent with measurements from Lake Geneva.<sup>8</sup>

To improve precision and validate the behaviour of MGe species, selected samples from a single depth in both reservoirs and inlet samples were reanalysed using a Ge-specific analytical method<sup>48</sup> with lower limits of detection. The results, shown in Table 2 and in the Supplementary Information Excel file, confirm the initial measurements. The MGe/DMGe ratio in these samples analysed with the Ge specific method was  $4.1 (\pm 0.4)$ , consistent with ratios observed in certified reference materials (NASS5, NASS7, CASS4 and CASS6),<sup>18</sup> Lake Geneva<sup>8</sup> and marine environments.<sup>49-51</sup>

Interestingly, the concentrations of MGe and DMGe in the Vrchlice reservoir were comparable to those in its inlet, and the same pattern was observed in Souš, where MGe was only detectable using the Ge-specific method (Table 2). Although the number of inlet samples was limited, this suggests that in-reservoir formation of MGe species is negligible. This is consistent with the fact that stocks of MeGe in Vrchlice reservoir remain constant throughout the year (Figure 4a) and are therefore not subject to variations due to water renewal or other processes. Furthermore, no elevated concentrations were found near the sediment–water interface or in bottom samples that were disturbed by contact of the sampler with the sediments. This provides additional evidence that methylation is not occurring in the sediments, in line with previous findings in Lake Geneva.<sup>8</sup>

## Conclusions

This study highlights the key role played by siliceous organisms in shaping the cycling of dissolved inorganic germanium (iGe) in freshwater systems. The contrasting behaviour observed in Vrchlice, where diatom activity drives biological uptake, and in Souš, where diatoms are virtually absent, highlight how biological presence can fundamentally alter iGe dynamics. While a relationship between iGe and iron remains plausible, it remains to be confirmed.

The elevated iGe concentrations at Souš are best explained by sediment diffusion, probably reflecting a legacy of historical germanium accumulation during periods of acid rain. This

mechanism highlights how past environmental conditions can leave persistent imprints on lake geochemistry.

Importantly, the contrasting dynamics of these two systems also reveal the limitations of using the Ge/Si molar ratio as a diagnostic tool. In environments where a single dominant process governs element cycling, the ratio can be informative. However, under the complex interplay of biological uptake, sediment release, hydrological variability and legacy deposition, as observed here, the interpretive power of the ratio is greatly diminished.

Finally, the application of a highly sensitive analytical method allowed the detection of methylated germanium species at very low concentrations. These compounds showed conservative behaviour in both reservoirs, with no evidence of *in situ* production within the sediments. This suggests a decoupling between the biogeochemical cycles of inorganic and methylated germanium, opening new questions about the sources and pathways of the latter in freshwater environments.

### Acknowledgements

The authors acknowledge the Czech Science Foundation (23-06530S), the Czech Academy of Sciences Premium Academiae, as well as the institutional support of the Czech Academy of Sciences (RVO: 68081715 and RVO: 67985874) and Strategy AV21 (VP20 – Water for life) for valuable support. We are indebted to Luděk Rederer (PLA) for providing us with data from PLA periodic monitoring and reservoirs' bathymetry, and to Petr Drahota for providing information on the geology of the Vrchlice area.

1  
2  
3  
4  
5  
6  
7  
8  
9  
10  
11  
12  
13  
14  
15  
16  
17  
18  
19  
20  
21  
22  
23  
24  
25  
26  
27  
28  
29  
30  
31  
32  
33  
34  
35  
36  
37  
38  
39  
40  
41  
42  
43  
44  
45  
46  
47  
48  
49  
50  
51  
52  
53  
54  
55  
56  
57  
58  
59  
60

Open Access Article. Published on 26 March 2026. Downloaded on 16/2/2026 6:03:14 AM.  
This article is licensed under a Creative Commons Attribution 3.0 Unported Licence.



## References

- 1 F. Melcher and P. Buchholz, Germanium. In: Gunn G. (ed) *Critical Metals Handbook*. BGS, AGU, Wiley, New York, 2014, p 177.
- 2 M. Filella and J.C. Rodriguez-Murillo, Less-studied TCE: are their environmental concentrations increasing due to their use in new technologies? *Chemosphere*, 2017, **182**, 605–616. doi:10.1016/j.chemosphere.2017.05.024.
- 3 U.S. Geological Survey, Mineral Commodity Summaries, January 2024. Available at: <https://pubs.usgs.gov/periodicals/mcs2024/mcs2024-germanium.pdf>; last accessed 08/01/2025.
- 4 M. Filella and J.C. Rodriguez-Murillo, Germanium in the environment: current knowledge and identification of gaps, *Soil & Environmental Health*, 2025, **3**, 100132. doi:10.1016/j.seh.2025.100132.
- 5 B. L. Lewis and H. P. Mayer, Biogeochemistry of methyl germanium in natural waters, *Metal Ions in Biological Systems*, 1993, **29**, 79–100.
- 6 B. L. Lewis, M. O. Andreae, P. N. Froelich and R.A. Mortlock, A review of the biogeochemistry of germanium in natural waters, *Sci. Total Environ.*, 1988, **73**, 107–120. doi:10.1016/0048-9697(88)90191-X
- 7 B. L. Lewis, M. O. Andreae and P. N. Froelich, Sources and sinks of methylgermanium in natural waters, *Mar. Chem.*, 1989, **27**, 179–200. doi:10.1016/0304-4203(89)90047-9
- 8 M. Filella and T. Matoušek, Germanium in Lake Geneva (Switzerland/France) along the spring productivity period, *Appl. Geochem.*, 2022, **143**, 105352, doi:10.1016/j.apgeochem.2022.105352.
- 9 L. Rederer and P. Ferbar, Vodárenská nádrž Vrchlice. Povodí Labe, Hradec Králové. 2017. Available online: [http://www.pla.cz/planet/public/dokumenty/publikace/2017\\_Vodarenske\\_zdroje.pdf](http://www.pla.cz/planet/public/dokumenty/publikace/2017_Vodarenske_zdroje.pdf) (accessed on 8 January 2026).

- 1  
2  
3  
4  
5  
6  
7  
8  
9  
10  
11  
12  
13  
14  
15  
16  
17  
18  
19  
20  
21  
22  
23  
24  
25  
26  
27  
28  
29  
30  
31  
32  
33  
34  
35  
36  
37  
38  
39  
40  
41  
42  
43  
44  
45  
46  
47  
48  
49  
50  
51  
52  
53  
54  
55  
56  
57  
58  
59  
60
- 10 J. Krasa, T. Dostal, A. Van Rompaey, J. Vaska and K. Vrana, Reservoirs' siltation measurements and sediment transport assessment in the Czech Republic, the Vrchlice catchment study, *Catena*, 2005, **64**, 348–362. doi:10.1016/j.catena.2005.08.015
- 11 J. Winterová, J. Krása, M. Bauer, N. Noreika and T. Dostál, Using WaTEM/SEDEM to model the effects of crop rotation and changes in land use on sediment transport in the Vrchlice Watershed, *Sustainability*, 2022, **14**, 5748. doi:10.3390/su14105748
- 12 R. Pažout, J. Sejkora and V. Šrein, Ag-Pb-Sb sulfosalts and Se-rich mineralization of Anthony of Padua Mine near Poličany—Model example of the mineralization of silver lodes in the historic Kutná Hora Ag-Pb ore district, Czech Republic. *Minerals*, 2019, **9**, 430. doi:10.3390/min9070430
- 13 J. Pobřísllová, Experimentální Povodí Jizerské Hory. Hydrologický Rok 2023. Český hydrometeorologický ústav, 2024. Available at: [https://intranet.chmi.cz/files/portal/docs/hydro/ohv/rocenkaOAH\\_2023.pdf](https://intranet.chmi.cz/files/portal/docs/hydro/ohv/rocenkaOAH_2023.pdf) (last accessed 8 January 2026)
- 14 J. Pobřísllová, Experimentální Povodí Jizerské Hory. Hydrologický Rok 2024. Český hydrometeorologický ústav, 2025. Available at: [https://intranet.chmi.cz/files/portal/docs/hydro/ohv/rocenkaOAH\\_2024.pdf](https://intranet.chmi.cz/files/portal/docs/hydro/ohv/rocenkaOAH_2024.pdf) (last accessed 8 January 2026)
- 15 Z. Hořická, T. Bímová, L. Procházková, E. Stuchlík and D. Vondrák, Biological recovery of reservoirs in the Jizera Mountains, the Czech Republic, from acidification, Chapter 7 in *ICP Waters report 112/2013*, 2013.
- 16 L. Macek and A. Grünwald, Influence of acid deposition on water quality in the Souš reservoir, *Water Sci. Technol.*, 1996, **33**, 285–290. doi:10.1016/0273-1223(96)00242-9
- 17 T. Matoušek, S. Adamová, M. Prokopová, M. Pivokonský, S. Musil and M. Filella, Simultaneous ultratrace analysis of antimony, arsenic and germanium species by Hydride Generation–Cryotrapping–ICP-MS/MS: Focus on antimony in freshwaters, *Spectrochim. Acta, Part B*, 2026 **240**, 107501, (2026). doi:10.1016/j.sab.2026.107501

- 1  
2  
3  
4  
5  
6  
7  
8  
9  
10  
11  
12  
13  
14  
15  
16  
17  
18 A. García-Figueroa, M. Filella and T. Matoušek, Speciation of germanium in environmental  
19 water reference materials by Hydride Generation and Cryotrapping in combination with  
20 ICP-MS/MS, *Talanta*, 2021, **225**, 121972. doi:10.1016/j.talanta.2020.121972.
- 21  
22  
23  
24  
25  
26  
27  
28  
29  
30  
31  
32  
33  
34  
35  
36  
37  
38  
39  
40  
41  
42  
43  
44  
45  
46  
47  
48  
49  
50  
51  
52  
53  
54  
55  
56  
57  
58  
59  
60
- 19 J. L. Weishaar, G. R. Aiken, B. A. Bergamaschi, M. S. Fram, R. Fujii and K. Mopper,  
Evaluation of specific ultraviolet absorbance as an indicator of the chemical composition  
and reactivity of dissolved organic carbon, *Environ. Sci. Technol.*, 2003, **37**, 4702–4708.  
doi:10.1021/es030360x
- 20 V. Chanudet and M. Filella, Submicron organic matter in a peri-alpine, ultra-oligotrophic  
lake, *Org. Geochem.*, 2007, **38**, 1146–1160. doi:10.1016/j.orggeochem.2007.02.011
- 21 E. Stuchlík, Z. Stuchlíková-Hořická, M. Prchalová, J. Křeček and J. Barica, Hydrobiological  
investigation of three acidified reservoirs in the Jizera Mountains, the Czech Republic,  
during the summer stratification, *Can. Tech. Rep. Fish. Aquat. Sci.*, 1997, **2155**, 56-64.
- 22 R. W. Battarbee, Diatom analysis and the acidification of lakes, *Phil. Trans. R. Soc. Land. B*,  
1984, **305**, 451–477. doi:10.1098/rstb.1984.0070
- 23 J. P. Smol, R. W. Battarbee, R. B. Davis and J. Meriläinen (editors), *Diatoms and Lake  
Acidity. Reconstructing pH from Siliceous Algal Remains in Lake Sediments*. Dr W. Junk  
Publishers, Dordrecht 1986.
- 24 R. B. Davis, Paleolimnological diatom studies of acidification of lakes by acid rain: An  
application of quaternary science, *Quat. Sci. Rev.*, 1987, **6**, 147–163. doi:10.1016/0277-  
3791(87)90031-X
- 25 J. Lewin, Silicon metabolism in diatoms. V. Germanium dioxide, a specific inhibitor of  
diatom growth, *Phycologia*, 1966, **6**, 1–12. doi:10.2216/i0031-8884-6-1-1.1
- 26 R. Shea and T. Chopin, Effects of germanium dioxide, an inhibitor of diatom growth, on the  
microscopic laboratory cultivation stage of the kelp, *Laminaria saccharina*, *J. Appl.  
Phycol.*, 2007, **19**, 27–32. doi:10.1007/s10811-006-9107-x
- 27 R. Rautenberger, Germanium dioxide as agent to control the biofouling diatom  
*Fragilariopsis oceanica* for the cultivation of *Ulva fenestrata* (Chlorophyta), *Botanica  
Marina*, 2024, **67**, 93–100. doi:10.1515/bot-2023-0075

- 1  
2  
3  
4  
5  
6  
7  
8  
9  
10  
11  
12  
13  
14  
15  
16  
17  
18  
19  
20  
21  
22  
23  
24  
25  
26  
27  
28  
29  
30  
31  
32  
33  
34  
35  
36  
37  
38  
39  
40  
41  
42  
43  
44  
45  
46  
47  
48  
49  
50  
51  
52  
53  
54  
55  
56  
57  
58  
59  
60
- 28 T. A. Safonova, V. V. Annenkov, E. P. Chebykin, E. N. Danilovtseva, Ye. V. Likhoshway and M. A. Grachev, Aberration of morphogenesis of siliceous frustule elements of the diatom *Synedraacus* in the presence of germanic acid, *Biochemistry-Moscow*, 2007, **72**, 1261–1270. doi:10.1134/S0006297907110132
- 29 A. K. Davis and M. Hildebrand, A self-propagating system for Ge incorporation into nanostructured silica, *Chem. Commun. (Camb)*, 2008, **37**, 4495–4497. doi:10.1039/b804955f
- 30 K. K. Bertine and E. D. Goldberg, Fossil fuel combustion and the major sedimentary cycle, *Science*, 1971, **173**, 233–235. doi:10.1126/science.173.3993.233
- 31 M. O. Andreae, J. T. Byrd and P. N. Froelich, Arsenic, antimony, germanium, and tin in the Tejo Estuary, Portugal: Modeling a polluted estuary, *Environ. Sci. Technol.*, 1983, **17**, 731–737. doi:10.1021/es00118a008
- 32 M. O. Andreae and P. N. Froelich Jr., Arsenic, antimony, and germanium biogeochemistry in the Baltic Sea, *Tellus*, 1984, **36B**, 101–117. doi:10.3402/tellusb.v36i2.14880
- 33 P. N. Froelich, G. A. Hambrick, M. O. Andreae, R. A. Mortlock and J.M. Edmond, The geochemistry of inorganic germanium in natural waters, *J. Geophys. Res.*, 1985, **90**, 1133–1141. doi:10.1029/JC090iC01p01133
- 34 R. A. Mortlock and P. N. Froelich, Continental weathering of germanium: Ge/Si in the global river discharge, *Geochim. Cosmochim. Acta*, 1987, **51**, 2075–2082. doi:10.1016/0016-7037(87)90257-2
- 35 A. A. Aguirre, L. A. Derry, T. J. Mills and S. P., Anderson, Colloidal transport in the Gordon Gulch catchment of the Boulder Creek CZO and its effect on C-Q relationships for silicon, *Water Resour. Res.*, 2017, **53**, 2368–2383. doi:10.1002/2016WR019730
- 36 Y. Han, Y. Huh and L. Derry, Ge/Si ratios indicating hydrothermal and sulfide weathering input to rivers of the Eastern Tibetan Plateau and Mt. Baekdu, *Chem. Geol.* 2015, **410**, 40–52. doi:10.1016/j.chemgeo.2015.06.001
- 37 O. Klein, T. Zimmermann, L. Hildebrandt and D. Pröfrock, Technology-critical elements in Rhine sediments - A case study on occurrence and spatial distribution, *Sci. Total Environ.*, 2022, **852**, 158464. doi:10.1016/j.scitotenv.2022.158464

- 1  
2  
3  
4  
5  
6  
7  
8  
9  
10  
11  
12  
13  
14  
15  
16  
17  
18  
19  
20  
21  
22  
23  
24  
25  
26  
27  
28  
29  
30  
31  
32  
33  
34  
35  
36  
37  
38  
39  
40  
41  
42  
43  
44  
45  
46  
47  
48  
49  
50  
51  
52  
53  
54  
55  
56  
57  
58  
59  
60
- 38 W. Davison, Iron and manganese in lakes, *Earth-Sci. Rev.*, 1993, **34**, 119–163.  
doi:10.1016/0012-8252(93)90029-7.
- 39 R. J. Murnane, B. Leslie, D. E. Hammond and R. F. Stallard, Germanium geochemistry in  
the Southern California Borderlands, *Geochim. Cosmochim. Acta*, 1989, **53**, 2873–2882.  
doi:10.1016/0016-7037(89)90164-6
- 40 D. E. Hammond, J. McManus, W. M. Berelson, C. Meredith, G. P. Klinkhammer and K. H.  
Coale, Diagenetic fractionation of Ge and Si in reducing sediments: The missing Ge sink  
and a possible mechanism to cause glacial/interglacial variations in oceanic Ge/Si, *Geochim.  
Cosmochim. Acta*, 2000, **64**, 2453–2465. doi:10.1016/S0016-7037(00)00362-8
- 41 S. L. King, P. N. Froelich and N. A. Jahnke, Early diagenesis of germanium in sediments of  
the Antarctic South Atlantic: In search of the missing Ge sink, *Geochim. Cosmochim. Acta*,  
2000, **64**, 1375–1390. doi:10.1016/S0016-7037(99)00406-8
- 42 S. N. Chillrud, F. L. Pedrozo, P. F. Temporetti, H. F. Planas and P. N. Froelich, Chemical  
weathering of phosphate and germanium in glacial meltwater streams: Effects of subglacial  
pyrite oxidation, *Limnol. Oceanogr.*, 1994, **39**, 1130–1140. doi:10.4319/lo.1994.39.5.1130
- 43 A. M. Scribner, A. C. Kurtz and O. A. Chadwick, Germanium sequestration by soil:  
Targeting the roles of secondary clays and Fe-oxyhydroxides, *Earth Planet. Sci. Lett*, 2006,  
**243**, 760–770. doi:10.1016/j.epsl.2006.01.051
- 44 M. Filella and J.C. Rodriguez-Murillo, Germanium in the ocean: relationships to silica. In:  
*Environmental Chemistry in Service of Life. Understanding the Self-Cleansing Capacity of  
Aquatic Systems through Environmental Biology and Chemistry*, Springer Nature  
Switzerland, Open Access eBook, 2016, accepted.
- 45 P. N. Froelich, V. Blanc, R. A. Mortlock and S. N. Chillrud, River fluxes of dissolved silica  
to the ocean were higher during glacials: Ge/Si in diatoms, rivers and oceans,  
*Paleoceanography*, 1992, **7**, 739–767. doi:10.1029/92PA02090
- 46 J. J. Baronas, D. E. Hammond, W M. Berelson, J. McManus and S. Severmann,  
Germanium–silicon fractionation in a river-influenced continental margin: The Northern  
Gulf of Mexico, *Geochim. Cosmochim. Acta*, 2016, **178**, 124–142.  
doi:10.1016/j.gca.2016.01.028

- 1  
2  
3  
4  
5  
6  
7  
8  
9  
10  
11  
12  
13  
14  
15  
16  
17  
18  
19  
20  
21  
22  
23  
24  
25  
26  
27  
28  
29  
30  
31  
32  
33  
34  
35  
36  
37  
38  
39  
40  
41  
42  
43  
44  
45  
46  
47  
48  
49  
50  
51  
52  
53  
54  
55  
56  
57  
58  
59  
60
- 47 R. J. Murnane and R. F. Stallard, Germanium and silicon in rivers of the Orinoco drainage basin, *Nature*, 1990, **344**, 749–752. doi:10.1038/344749a0
- 48 A. C. Kurtz, L. A. Derry and O. A. Chadwick, Germanium-silicon fractionation in the weathering environment, *Geochim. Cosmochim. Acta*, 2002, **66**, 1525–1537. doi:10.1016/S0016-7037(01)00869-9
- 49 K. Jin, Y. Shibata and M. Morita, Determination of germanium species by hydride generation-inductively coupled argon plasma mass spectrometry, *Anal. Chem.*, 1991, **63**, 986–989. doi:10.1021/ac00010a010
- 50 M. J. Ellwood, and W. A. Maher, An automated hydride generation-cryogenic trapping-ICP-MS system for measuring inorganic and methylated Ge, Sb and As species in marine and fresh waters, *J. Anal. At. Spectrom.*, 2002, **17**, 197–203. doi:10.1039/b109754g
- 51 M. J. Ellwood, and W. A. Maher, Germanium cycling in the waters across a frontal zone: the Chatham Rise, New Zealand, *Mar. Chem.*, 2003, **80**, 145–159. doi:10.1016/S0304-4203(02)00115-9

Figure 1. Location of the two reservoirs. Coordinates are given in the text.

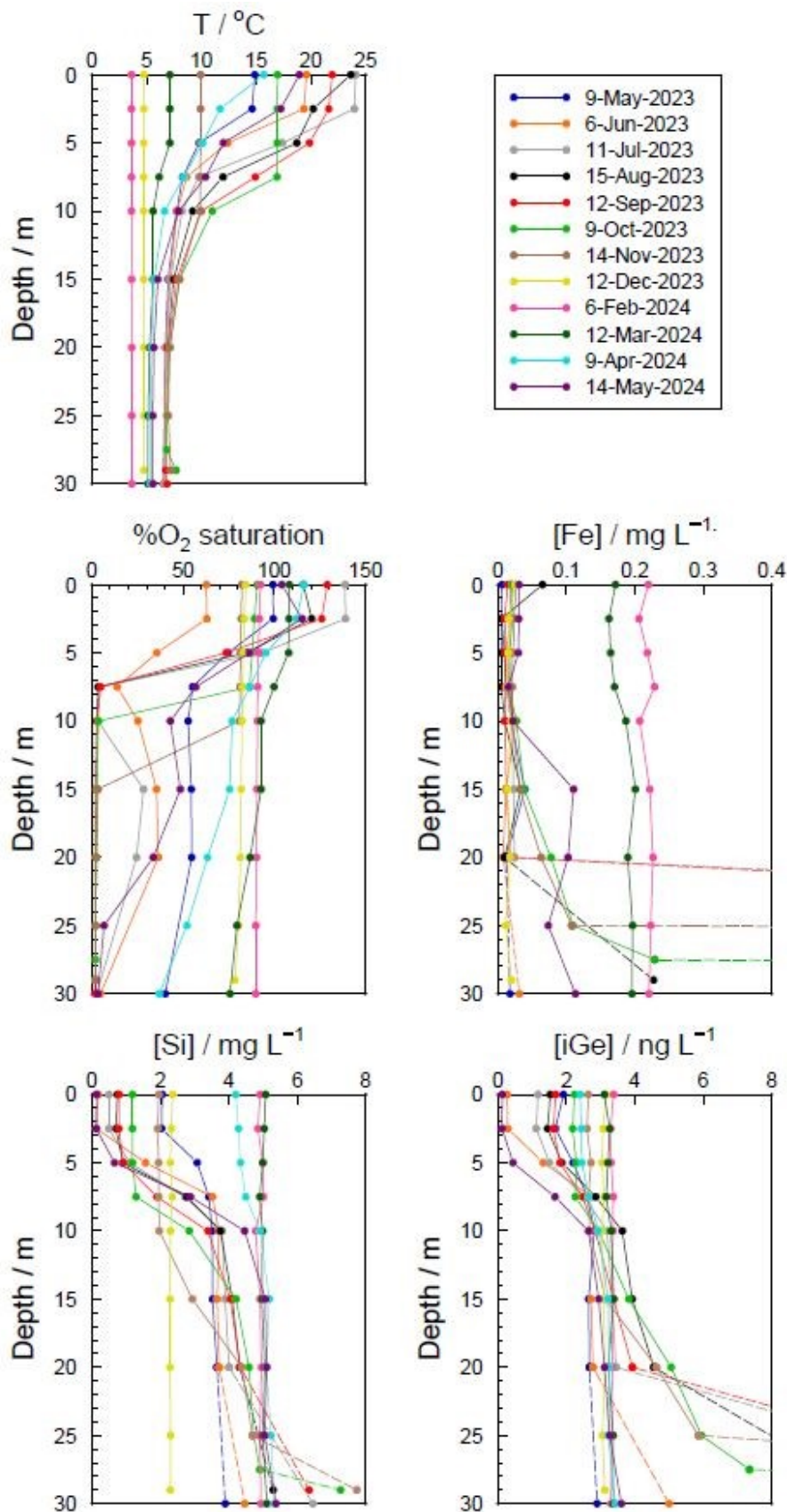


Figure 2. Vertical profiles of temperature, percentage of O<sub>2</sub> saturation, iron, dissolved silicon and dissolved germanium in Vrchlice reservoir (49.9270392N, 15.2270806E) from May 2023 to May 2024. Vrchlice was not sampled in December due to winter conditions. The dashed lower parts of some profiles correspond to samples where the sediments were disturbed during sampling.

1  
2  
3  
4  
5  
6  
7  
8  
9  
10  
11  
12  
13  
14  
15  
16  
17  
18  
19  
20  
21  
22  
23  
24  
25  
26  
27  
28  
29  
30  
31  
32  
33  
34  
35  
36  
37  
38  
39  
40  
41  
42  
43  
44  
45  
46  
47  
48  
49  
50  
51  
52  
53  
54  
55  
56  
57  
58  
59  
60

Open Access Article. Published on 26 March 2026. Downloaded on 4/16/2026 6:06:31 AM.  
This article is licensed under a Creative Commons Attribution 3.0 Unported Licence.  


Environmental Science: Processes & Impacts Accepted Manuscript



1  
2  
3  
4  
5  
6  
7  
8  
9  
10  
11  
12  
13  
14  
15  
16  
17  
18  
19  
20  
21  
22  
23  
24  
25  
26  
27  
28  
29  
30  
31  
32  
33  
34  
35  
36  
37  
38  
39  
40  
41  
42  
43  
44  
45  
46  
47  
48  
49  
50  
51  
52  
53  
54  
55  
56  
57  
58  
59  
60

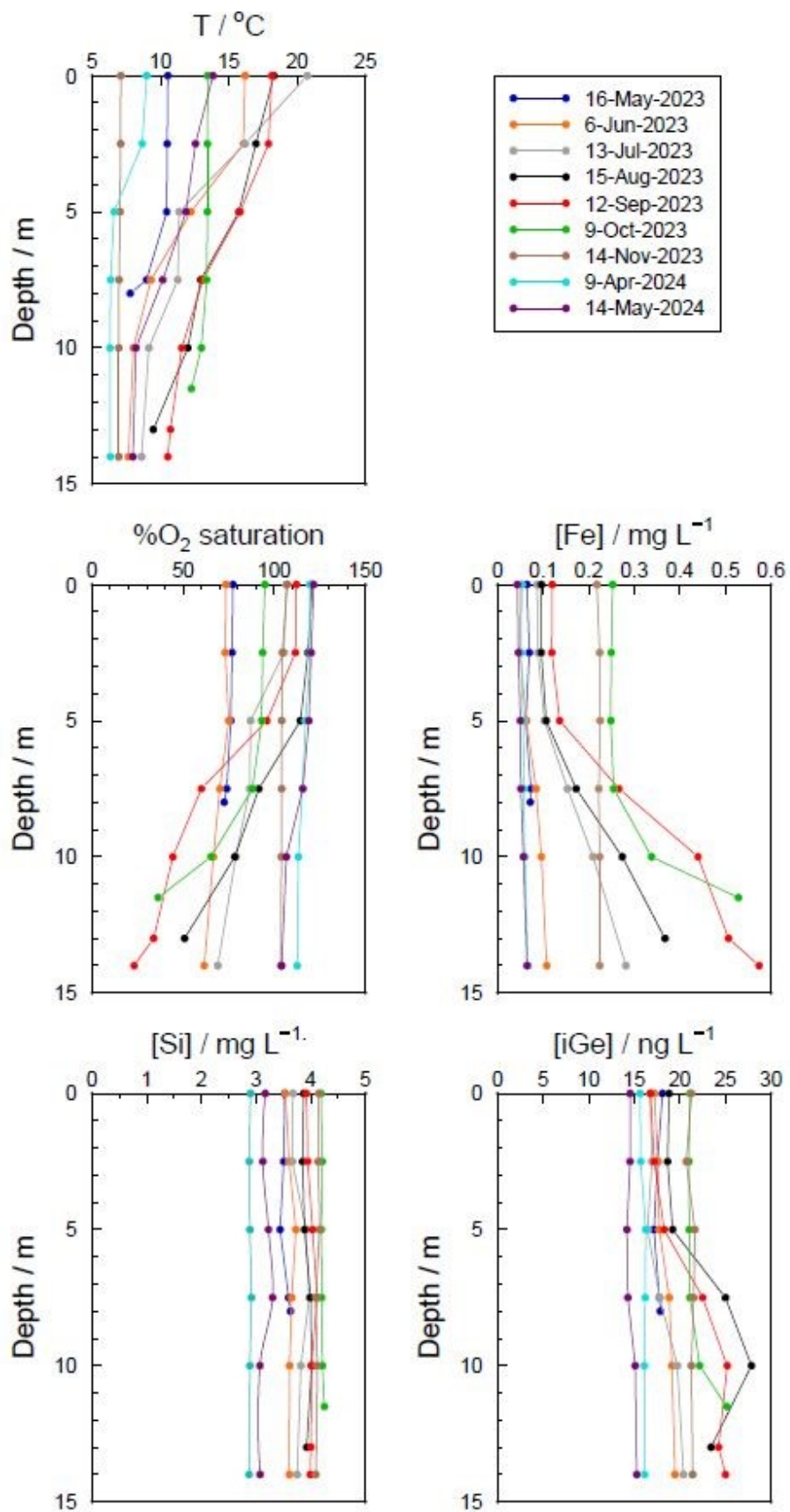
Open Access Article. Published on 26 March 2026. Downloaded on 16/2/2026 6:03:11 AM.  
This article is licensed under a Creative Commons Attribution 3.0 Unported Licence.

Figure 3. Vertical profiles of temperature, percentage of O<sub>2</sub> saturation, iron, dissolved silicon and dissolved germanium in Souš reservoir (50.7911378N, 15.3183094E) from May 2023 to May 2024. Souš was not sampled from December 2023 to March 2024 due to winter conditions.

1  
2  
3  
4  
5  
6  
7  
8  
9  
10  
11  
12  
13  
14  
15  
16  
17  
18  
19  
20  
21  
22  
23  
24  
25  
26  
27  
28  
29  
30  
31  
32  
33  
34  
35  
36  
37  
38  
39  
40  
41  
42  
43  
44  
45  
46  
47  
48  
49  
50  
51  
52  
53  
54  
55  
56  
57  
58  
59  
60

Open Access Article. Published on 26 March 2026. Downloaded on 4/16/2026 6:06:31 AM.  
This article is licensed under a Creative Commons Attribution 3.0 Unported Licence.





1  
2  
3  
4  
5  
6  
7  
8  
9  
10  
11  
12  
13  
14  
15  
16  
17  
18  
19  
20  
21  
22  
23  
24  
25  
26  
27  
28  
29  
30  
31  
32  
33  
34  
35  
36  
37  
38  
39  
40  
41  
42  
43  
44  
45  
46  
47  
48  
49  
50  
51  
52  
53  
54  
55  
56  
57  
58  
59  
60

Open Access Article. Published on 26 May 2026. Downloaded on 4/16/2026 6:03:11 AM.  
This article is licensed under a Creative Commons Attribution 3.0 Unported Licence.

Figure 4. Vrchlice (a) and Souš (b) water volumes (blue), 20 days water renewal (green) and standing stocks of iGe (magenta) over 2023–2024. MeGe standing stocks (violet) are also shown for Vrchlice. The relative error in the values of standing stocks mainly reflects the error of the analytical method, which lies between 3% and 5%.<sup>17</sup> Red points show the sampling dates.

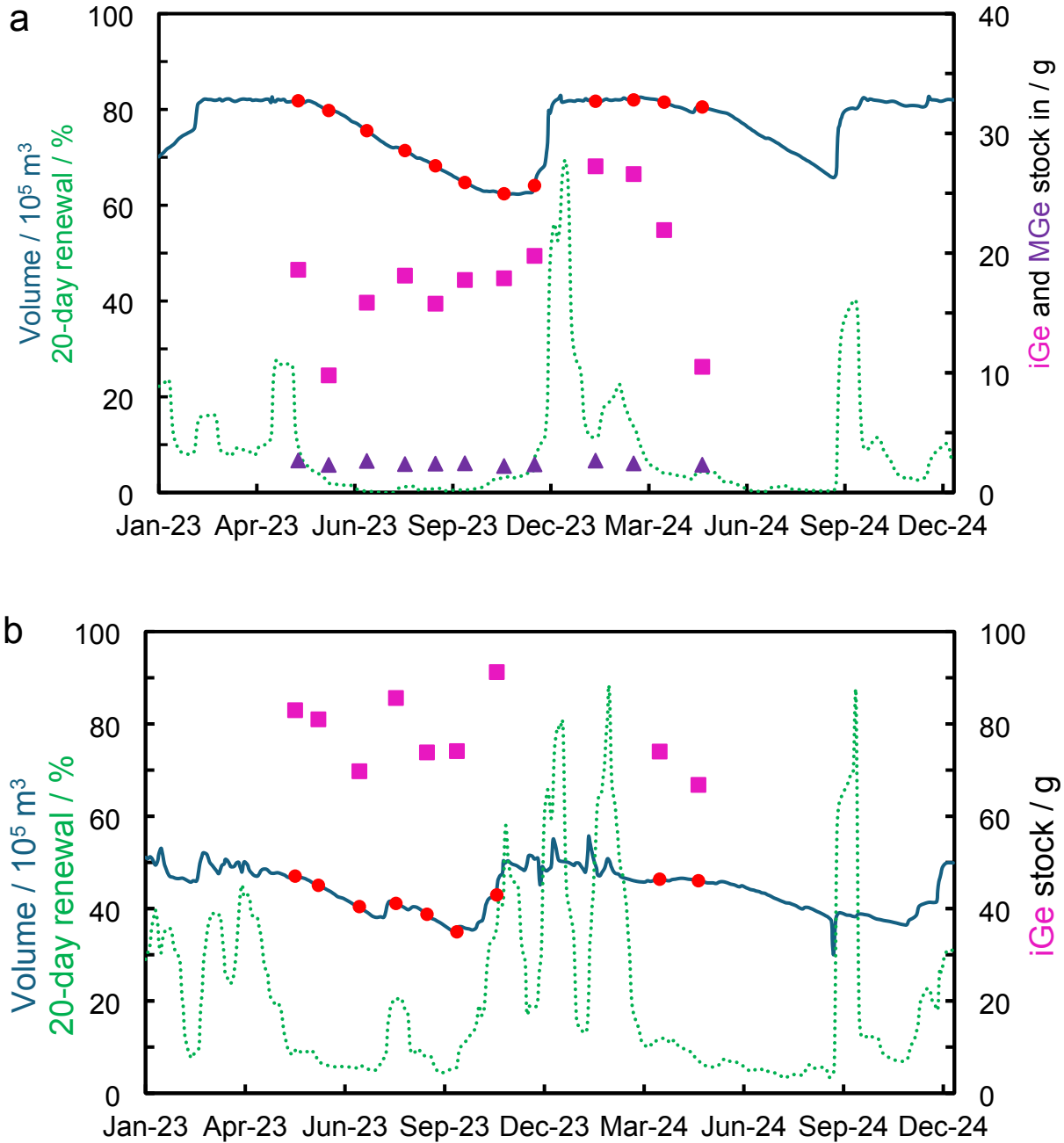

 1  
2  
3  
4  
5  
6  
7  
8  
9  
10  
11  
12  
13  
14  
15  
16  
17  
18  
19  
20  
21  
22  
23  
24  
25  
26  
27  
28  
29  
30  
31  
32  
33  
34  
35  
36  
37  
38  
39  
40  
41  
42  
43  
44  
45  
46  
47  
48  
49  
50  
51  
52  
53  
54  
55  
56  
57  
58  
59  
60

Figure 5. Seasonal evolution phytoplankton biomass in Souš (a) and in Vrchlice (b) reservoirs. The same colour codes apply to both figures.

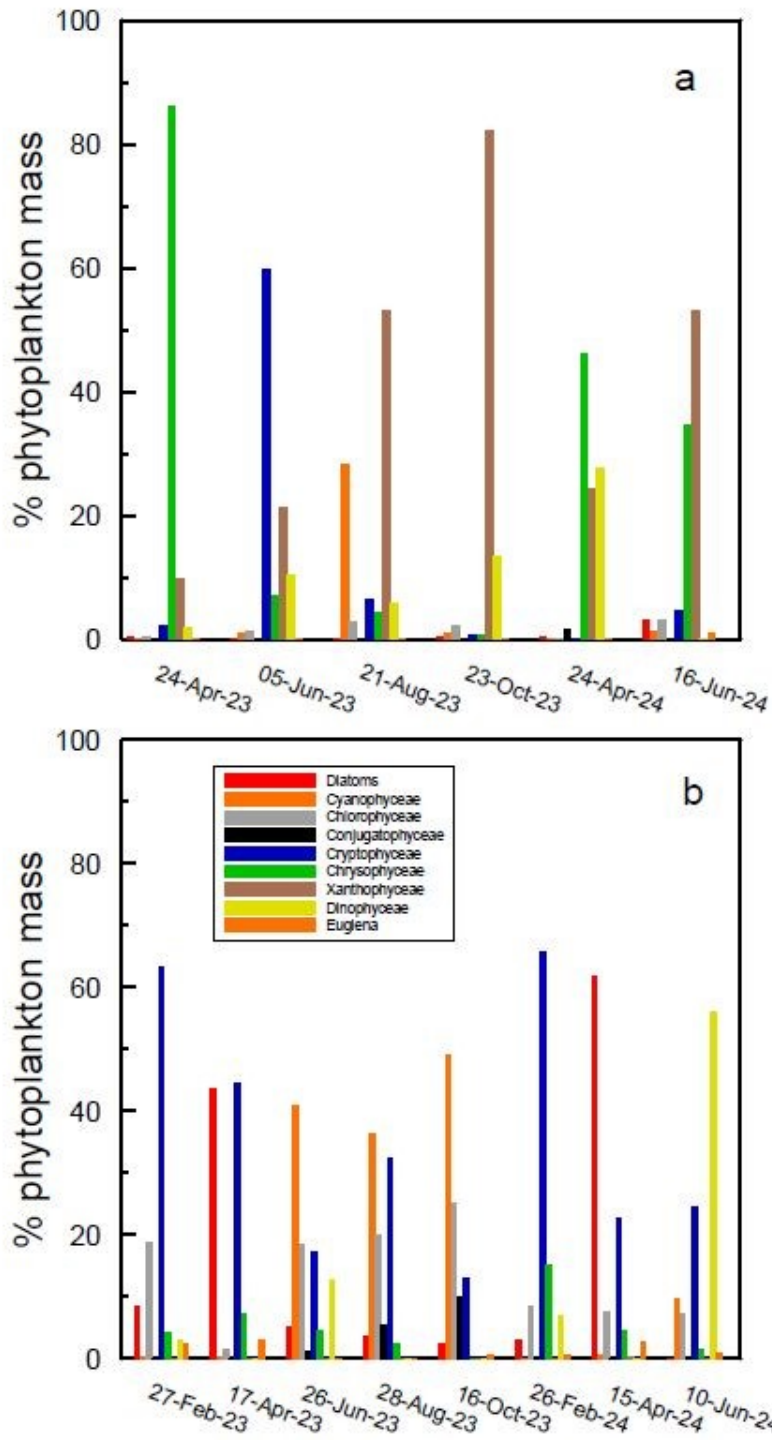


Figure 6. Vertical profiles of methylgermanium and dimethylgermanium in Vrchlice reservoir (49.9270392N, 15.2270806E) from May 2023 to May 2024.

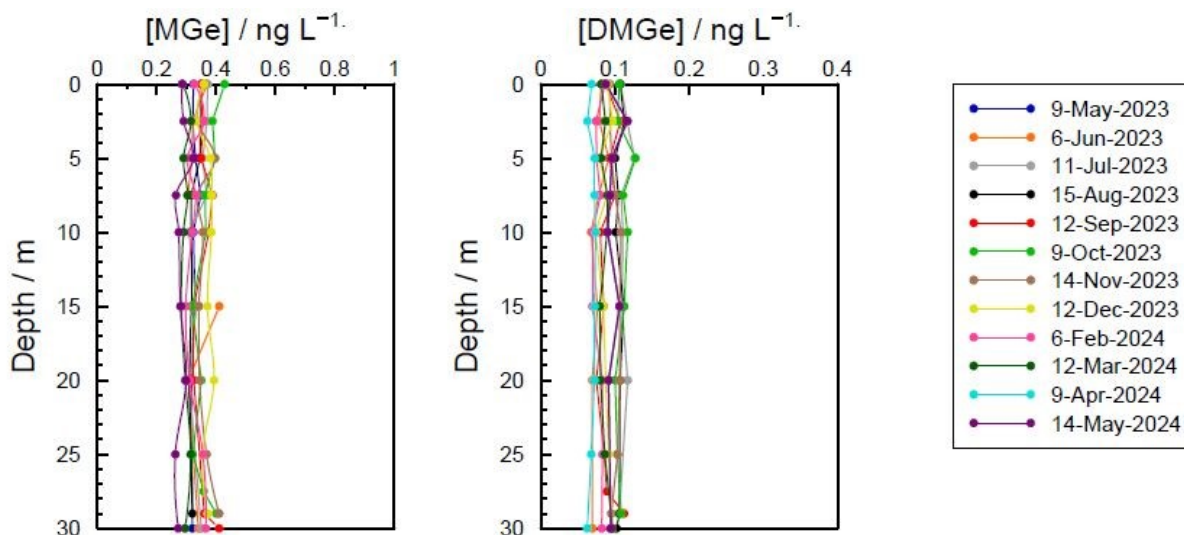


Table 1. Main reservoirs' characteristics


		Souš	Vrchlice
River	Name	Černá Desná	Vrchlice
	Catchment area (km <sup>2</sup> )	13.77	97.4
	Mean flow (m <sup>3</sup> s <sup>-1</sup> )	0.505	0.396
	100 year flood flow (m <sup>3</sup> s <sup>-1</sup> )	89.8	50.5
Reservoir	Water surface (ha)	68.7	93.5
	Active storage (m <sup>3</sup> )	4.585 mil	7.890 mil
	Flood storage (m <sup>3</sup> )	2.476 mil	1.463 mil
	Reservoir capacity (total) (m <sup>3</sup> )	7.480 mil	9.785 mil
	Population served	70'000	50'000

Table 2. Concentrations of Ge species (in ng L<sup>-1</sup>) in Vrchlice and Souš and their inlets from 14 May 2024, reanalysed by using the Ge specific method.<sup>48</sup>

	iGe	MGe	DMGe
Vrchlice, 5 m depth	0.8	0.32	0.08
Vrchlice inlet in Malešov (IV1)	5.1	0.42	0.11
Souš, 2.5 m depth	15.5	0.05	<0.02
Souš, Černá Desná inlet (IS1)	10.1	0.04	<0.02
Souš, Bílá Desná inlet (IS2)	6.6	0.05	<0.02

1  
2  
3  
4  
5  
6  
7  
8  
9  
10  
11  
12  
13  
14  
15  
16  
17  
18  
19  
20  
21  
22  
23  
24  
25  
26  
27  
28  
29  
30  
31  
32  
33  
34  
35  
36  
37  
38  
39  
40  
41  
42  
43  
44  
45  
46  
47  
48  
49  
50  
51  
52  
53  
54  
55  
56  
57  
58  
59  
60

Open Access Article. Published on 26 March 2026. Downloaded on 4/16/2026 6:06:51 AM.  
This article is licensed under a Creative Commons Attribution 3.0 Unported Licence.



All data are provided in the Supplementary Information Excel file

1  
2  
3  
4  
5  
6  
7  
8  
9  
10  
11  
12  
13  
14  
15  
16  
17  
18  
19  
20  
21  
22  
23  
24  
25  
26  
27  
28  
29  
30  
31  
32  
33  
34  
35  
36  
37  
38  
39  
40  
41  
42  
43  
44  
45  
46  
47  
48  
49  
50  
51  
52  
53  
54  
55  
56  
57  
58  
59  
60

Open Access Article. Published on 26 March 2026. Downloaded on 4/16/2026 6:06:31 AM.  
This article is licensed under a Creative Commons Attribution 3.0 Unported Licence.  


Environmental Science: Processes & Impacts Accepted Manuscript